Clim. Past Discuss., 9, 2889–2928, 2013
www.clim-past-discuss.net/9/2889/2013/
doi:10.5194/cpd-9-2889-2013


Climate of the Past
Discussions
Open Access



Discussion Paper | Discussion Paper | Discussion Paper | Discussion Paper |



# Mid and late Holocene dust deposition in western Europe: the Misten peat bog (Hautes Fagnes – Belgium)

**M. Allan[1], G. Le Roux[2,3], N. Piotrowska[4], J. Beghin[5], E. Javaux[5], M. Court-Picon[5,6], N. Mattielli[7], S. Verheyden[6,8], and N. Fagel[1]**

[1]AGEs, Department of Geology, University of Liege, B18 Sart Tilman, Liège, Belgium
[2]Université de Toulouse; INP, UPS; EcoLab (Laboratoire Ecologie Fonctionnelle et Environnement); ENSAT, Avenue de l'Agrobiopole, 31326 Castanet Tolosan, France
[3]CNRS; EcoLab; 31326 Castanet Tolosan, France
[4]Department of Radioisotopes, GADAM Centre of Excellence, Institute of Physics, Silesian University of Technology, Gliwice, Poland
[5]Palaeobiogeology–Palaeobotany–Palaeopalynology, Department of Geology, University of Liege, Belgium
[6] Royal Belgian Institute of Natural Sciences, Earth and Life History Division, Vautier street, 1000 Brussels, Belgium
[7]G-Time, Dept. Earth and Environmental Sciences, Université Libre Bruxelles ULB, Belgium
[8]Collaborator of the Vrije Universiteit Brussel, Belgium

Received: 22 April 2013 – Accepted: 10 May 2013 – Published: 29 May 2013

Correspondence to: M. Allan (mallan@doct.ulg.ac.be)

Published by Copernicus Publications on behalf of the European Geosciences Union.





CPD
9, 2889–2928, 2013

## Abstract

Dust deposition in southern Belgium is estimated from the geochemical signature of an ombrotrophic peatland. The Rare Earth Elements (REE) and lithogenic elements concentrations, as well as Nd isotopes, were determined by HR-ICP-MS and MC-ICP-MS respectively, in along a ~6 m peat section covering 5300 yr, from 30 BC to 5300 BC dated by the $^{14}C$ method. Changes in REE concentration in the peat correlate with those of Ti, Al, Sc and Zr that are lithogenic conservative elements, suggesting that REE are immobile in the studied peat bogs and can be used as tracers of dust deposition. Peat humification and testate amoebae were used to evaluate hydroclimatic conditions. The range of dust deposition varied from 0.03 to 4.0 $g\,m^{-2}\,yr^{-1}$. The highest dust fluxes were observed from 800 to 600 BC and from 3200 to 2800 BC and correspond to cold periods. The $\varepsilon$Nd values show a large variability of −5 to −13, identifying three major sources of dusts: local soils, distal volcanic and desert particles.

## 1 Introduction

The Holocene period appears as a relatively stable climatic period compared to Quaternary glacial/interglacial variations. However recent high-resolution studies have emphasized many climatic oscillations over the last 11 500 yr (e.g., Mayewski et al., 2004; Wanner et al., 2008, 2011). The Holocene climate variability was tentatively attributed to orbital forcing, volcanic, and/or solar activity (Wanner et al., 2008). Several climatic proxies (e.g., $\delta^{18}O$, $\delta^{13}C$, $\delta^{14}C$, $^{10}Be$, REE content, pollen, dust, humification) have been measured in different geological archives such as peat (e.g., Blackford, 2000; Marx et al., 2009, 2011; Roos-Barraclough et al., 2002; Shotyk et al., 2001, 2002; Spakota et al., 2007), speleothems (e.g., Bar-Matthews, 1997; Niggeman et al., 2003; Verheyden et al., 2008, 2012), ice cores (e.g., Bond et al., 2001; Delmonte et al., 2002; Gabrielli et al., 2010; Thompson et al., 2002), and lake sediments (e.g., Magny, 2004; Sirocko et al., 2013), to reconstruct past climate changes over the Holocene. In Europe, the Holocene was defined as a typical interglacial period with climate oscillations at various time scales, i.e. millennial, centennial, and decadal. On the millennial timescales, the period from 9000 to 5000 yr BP (7000 to 3000 BC) called "Holocene Climatic Optimum" in the Northern Hemisphere, is the warmest period in Greenland (Jonhsen et al., 2001) and in Scandinavia (Heikkila and Seppa, 2003). The period from 5000–6000 yr BP (3000–4000 BC) to pre-industrial time corresponds to the Subboreal and Subatlantic and is called "Neoglacial" with a progressive temperature decline and glacier advances (Wanner et al., 2008, 2011).

Atmospheric dusts are an important part of the global climate system, and play an important role in the marine (Meskhidze et al., 2003) and terrestrial (Goudie and Middleton, 2006) biogeochemical cycles as major and trace nutrient elements. Reconstruction of dust composition and fluxes is crucial to help understanding Holocene climate variability as well as ongoing biogeochemical cycles. In the recent years, the link between Holocene climate and atmospheric dust deposition was intensively studied (e.g., Gabrielli et al., 2010; Lambert et al., 2012; Marx et al., 2011; Sapkota et al., 2007; Thompson et al., 2003). Climate (dry and/or wet conditions) influences the intensity of the transport of air particles and their abundance (Goudie, 2001). Dust particles can be transported for thousands of kilometres before thier deposition (Grousset et al., 2003). The principal sources of atmospheric dust are the world's deserts, and arid and semi-arid areas including North and South Africa, the Middle East and Asia, and Australia (Grousset and Biscaye, 2005). Dust deposition depends on several factors among which the dust concentration in the atmosphere and the vegetation cover (Lawrence and Neff, 2009). Local and regional anthropogenic sources may also influence the dust deposition (Tegen et al., 2004).

Ice cores have been used to reconstruct past dust deposition (Delmonte et al., 2002; Gabrielli et al., 2010; Lambert et al., 2008, 2012; Thompson et al., 2003), as well as speleothems (e.g. Frumkin and Stein, 2004). To complete the dust record, peat bogs present a large worldwide distribution on the continent. Since they receive only atmospheric input of particles, they are excellent records of atmospheric dust deposition





CPD
9, 2889–2928, 2013

(e.g., Aubert et al., 2006; Le Roux et al., 2012; Shotyk et al., 1998, 2002). In recent decades, a range of organic (e.g., plant macrofossils, peat humification, testate amoebae and pollen) and inorganic (e.g., particle size, mineralogy, and chemistry of atmospheric mineral dust) proxies has been used in peat bogs to trace past changes in temperature and precipitation (Chambers et al., 2011; Roos-Barraclough et al., 2002; Shotyk et al., 2001). However, only few studies address dust flux dealing reconstructions in peat cores (e.g., Kylander et al., 2007; Le Roux et al., 2012; Marx et al., 2005, 2009; Sapkota et al., 2006; Shotyk et al., 1998). The chemistry of atmospheric dusts particles trapped in the peat bogs can be used to distinguish between local, regional and hemispheric dust input related to climate changes (e.g., Krachler et al., 2003; Kamanov et al., 2009; Muller et al., 2007; Sapkota et al., 2006; Shotyk et al., 2002). In general, the mineralogy and the chemical and isotopic composition of the deposited dust should be similar to dust source material (Aubert et al., 2006; Roos-Barraclough et al., 2002; Spakota et al., 2006). However, the influence of dust on climate remains a poorly quantified and actively changing element of the Earth's climate system (Maher et al., 2010).

In this study a continuous dust record for the period between 5300 BC and 30 BC is produced from a Belgian ombro/minerotrophic bog. Main aims are (1) to reconstruct the changes in atmospheric dust deposition using Al, Ti, Sc, Zr, and REE elements; (2) to determine dust sources using REE content and Nd isotopes; (3) to characterize the relationship between dust flux and climatic variability during the mid and late Holocene through a comparison of dust records from peat bogs and ice cores in the Northern Hemisphere.





CPD
9, 2889–2928, 2013

## 2 Material and methods

### 2.1 Sampling and preparation

In February 2008, a peat core (MIS-08-01b, 750 cm) was collected from the Misten site in the Hautes-Fagnes Plateau, Belgium (Fig. 1). The top 100 cm was sampled by using a titanium Wardenaar corer (Wardenaar, 1987) from the University of Heidelberg. The lower peat was cored with a Belorussian corer (Belokopytov, 1955). We focused mainly our study on the prehistoric dust variability in the 135–750 depth intervals that represents ~5300 yr (from 5300 BC to 30 BC). Core sub-samples of 1 cm thick slices has been taken according to the protocol defined by Givelet et al. (2004). In Misten peat, Ca/Mg ratios, Sr concentration, and testate amoebae assemblages were used to distinguish between the ombrotrophic and minerotrophic peat section (Payne, 2011; Shotyk et al., 1996, 2001). The peat bog is ombrotrophic (receiving inputs exclusively or quasi-exclusively from the atmosphere) for the upper 6.8 m and minerotrophic for the lower interval (from 6.8 to 7.5 m).

### 2.2 Ash content and humification

To identify the content of mineral matter defined as "ash content", for all peat samples ($n = 420$), 0.1 to 1 g of dried peat was heated at 550 °C during 6 h to remove all organic matter by combustion (Chambers et al., 2011). The humification degree was estimated by the colorimetric method on peat alkaline extracts (Chambers et al., 2011) with a spectrophotometer for absorbance measurement at 540 nm available at the Liège University (Belgium).

### 2.3 Chemical analyses

Titanium (Ti), Aluminium (Al), Zirconium (Zr), Sc and Rare Earth Elements (REE) concentrations have been measured in the peat core every four centimetres ($n = 170$) by High Resolution Inductively Coupled Plasma Mass Spectroscopy (HR-ICP-MS Thermo





CPD
9, 2889–2928, 2013

Element XR) at the Observatoire Midi-Pyrénées in Toulouse (France) after complete digestion with a mixture of $HNO_3$-HF-$H_2O_2$ in Savillex® beakers on a hot plate in a clean room (class 100). The standards (*ICHTJ* CTA-OTL-1 Oriental Tobacco Leaves, *NIST* Tomato Leaves 1573 and *IAEA* Lichen 336) were analyzed to assess the external analytical reproducibility.

Fifty-eight samples were prepared for Nd isotopes (Table 1). About 200 mg of each sample was ashed at 550 °C during 6 h, to remove all organic matter (Chambers et al., 2011). The dried organic free samples were dissolved in a mixture of concentrated $HNO_3$ and HF in a proportion of 1 : 4 heated at 125 °C for 48 h. After drying, 2 mL of 6M HCl were added to ensure complete digestion and the solutions were evaporated. For separation of alkalis (e.g., Ca, Rb, Sr) and REE, the samples were dissolved in 2 mL of 1M HCl and passed on Bio-Rad columns filled with AG50W-X8 200 mesh resin (Ali and Srinivasan, 2011). Nd isotopes were isolated by passing the solution on Quartz columns filled with HDEHP resin. The samples were redissolved in 1.5 mL 0.05M $HNO_3$ before Nd isotopes measurement. The Nd isotopic ratios were measured by MC-ICP-MS (Multi Collector–Inductively Coupled plasma Mass Spectrometry, Nu Plasma), at G-Time Laboratory (Université Libre de Bruxelles). During the analysis, the Nd Rennes standard ($^{143}Nd/^{144}Nd = 0.511961 \pm 0.000008$, Chauvel and Blichert-Toft, 2001) was systematically run every two samples in order to control the instrument drift. The mean values obtained for the Nd Rennes standard were stable during the analysis sessions: $^{143}Nd/^{144}Nd = 0.511945 \pm 0.00002$ ($2\sigma$, $n \approx 150$), $^{145}Nd/^{144}Nd = 0.348404 \pm 0.000012$, $^{146}Nd/^{144}NdNd = 0.721598 \pm 0.000051$. Nd Rennes values are in agreement with the long term laboratory value [$n = 750$, $^{143}Nd/^{144}Nd = 0.511946 \pm 0.00003$]. The Nd isotopes and epsilon Nd are given in Table 1. Epsilon Neodymium ($\varepsilon$Nd) was calculated according to DePaolo al. (1976):

$$\varepsilon\text{Nd} = \left(\frac{(143\text{Nd}/144\text{Nd})}{0.512638} - 1\right) \times 10\,000$$

where 0.512638 corresponds to the chondritic uniform (CHUR).





CPD
9, 2889–2928, 2013

The $^{143}Nd/^{144}Nd$ ratios vary between 0.51184 and 0.51269 ($-13 < \varepsilon Nd < -5$, Fig. 3), whereas Sm/Nd ratios range from 0.1053 and 0.1398 (Table 1).

### 2.4 Testate amoebae

The hydrological conditions strongly control the occurrence and relative abundance of different testate amoeba species on peatlands (Charman et al., 2000). By analysing testate amoebae community changes over a peat profile, it is possible to quantitatively and qualitatively reconstruct changing mire surface wetness (Booth et al., 2004; Lamentowicz et al., 2008; Sillasoo et al., 2007).

Testate amoebae were isolated from Misten peat by a wet sieving procedure (Booth et al., 2010). One hundred individuals tests were counted for each sample ($n = 130$). The identification is done according to Charman et al. (2000) and Payne and Mitchell (2009). For a better visualization of wet and dry periods, the testate amoebae were classified according to their affinity with wet or dry conditions (Charman et al., 2000). Slides are scanned at 10 to 40 × magnification, by using standard optical light microscopy. The relative abundance of each species was calculated as a percentage of the total number of counted tests.

### 2.5 Radiocarbon dating

Radiocarbon ages were obtained on macrofossil samples (stems, branches or leaves of plant material) extracted under a binocular microscope. Samples were prepared at the GADAM Centre (Silesian University of Technology, Gliwice, Poland), according to the protocol described by Piotrowska et al. (2011) and Piotrowska (2013), and measured by Acceleration Mass Spectrometry (AMS). Radiocarbon dates ($n = 15$, Table 2) were processed using the "Bacon" software (Blaauw and Christen, 2011) to establish an age-depth model as well as an age range for each slice of peat (Fig. 2). The curve IntCal09 was used for calibration (Reimer et al., 2009). The age-depth model was calculated for 600 cm of studied peat core. The priors for accumulation rate were set as





CPD
9, 2889–2928, 2013

a gamma distribution with a mean of 10 yr $cm^{-1}$, shape 2. The accumulation variability was set with a beta distribution with strength of 4 and a mean of 0.7.

## 3 Results

### 3.1 Density, ash content and humificatio

The density of the Misten peat core from 135 to 750 cm-deep ranges between 0.01 and 0.12 g $cm^{-3}$. The ash content varies between 0.1 and 2.4 %. The humification degree varies between 25 and 80 % (Fig. 3). From 135 to 550 cm (ombrotrophic section), the highest density corresponds to the more humified peat sections ($r = -0.5$). This similarity can be explained by plant breakdown during the peat decomposition (Roos-Barraclough et al., 2002). In the lower peat section (below 680 cm, minerotrophic peat), the ash content progressively increases in parallel with the density ($r = 0.4$), towards the bottom of the core. The intermediate peat section (from 550 to 680 cm) is characterised by lower values of ash content and humification (Fig. 3).

### 3.2 Elemental concentrations

The conservative elements (Al, Sc, Ti, Zr) and REE concentration profiles in the Misten core are very similar (Fig. 4). We report La and Nd as Light REE (LREE), Sm and Eu as Middle REE (MREE) and Yb and Lu as Heavy REE (HREE) (Fig. 4). The REE concentrations remain relatively low and constant between 550 and 680 cm. They increase by a factor of 3 to 5 above 500 cm and below 680 cm (Fig. 4). The parallel trends between REE profiles with Al, Ti and Zr which are conservative elements (e.g. Aubert et al., 2006; Shotyk et al., 1998, 2001) attest that REE are not affected by any diagenetic processes. This observation confirms that the complete atmospheric REE pattern is preserved in Misten bog.





CPD
9, 2889–2928, 2013

### 3.3 Dust flux

According to Shotyk et al. (2002), the dust flux can be calculated using a conservative element concentration ($\mu g\, g^{-1}$) in the bulk peat compared to its occurrence in the Upper Continental Crust (UCC), the density of the peat ($g\, cm^{-3}$) and the peat accumulation rate ($cm\, yr^{-1}$):

$$\text{Dust flux}(g\, m^{-2}\, yr^{-1}) = ([\text{element}]_{\text{sample}}/[\text{element}]_{\text{UCC}}) \times \text{density} \\ \times \text{accumulation rate} \times 10\,000$$

The dust flux was calculated using Ti, Al, Zr, and $\sum$REE (Fig. 5). The four dust flux profiles are very similar ($r > 0.75$, $n = 170$). This similarity is explained by the positive correlation between Ti, Al, Zr, and $\sum$REE concentrations and by the fact that a main part of the dust input has a similar composition than the average upper continental crust (UCC). The dust flux profiles are very similar but their absolute values is depend on the reference element used (e.g. Ti, Al, Zr) to calculate it. The highest dust fluxes were observed from 800 to 600 BC (2–4.5 $g\, m^{-2}\, yr^{-1}$) and from 3200 to 2800 BC (1–2.4 $g\, m^{-2}\, yr^{-1}$).

### 3.4 Chronology of peat accumulation

The ranges of calibrated radiocarbon ages of dated peat layers are presented in Table 2. The age-depth model (Fig. 2) covers the period from ca. 30 BC to 5300 BC. The age model reveals a relatively constant peat accumulation rate, with an average value of ca. 0.11 $mm\, yr^{-1}$. Consequently, the analysed of 1 cm thick samples represents ca. 8.7 yr each, which limits the resolution of the dust flux reconstruction.

### 3.5 Testate amoebae

One hundred testate amoeba taxa were identified in the Misten peatland core. Six assemblage zones were defined and presented in Table 3. The fluctuations were primarily





CPD
9, 2889–2928, 2013

driven by changes in the relative abundance of *Amphitrema flavum*, *Difflugia pulex* and *Amphitrema wrightianum*.

## 4 Discussion

### 4.1 REE distribution pattern

The REE variations in the Misten peat core, normalized by the mean Upper Crust Continental values (UCC, Taylor and McLennan, 1985), are presented in three groups (Fig. 6) as based on the peat core stratigrapgy (ombrotrophic, minerotrophic, transition). The first group are represents the mean $REE_{UCC}$ values of the Misten ombrotrophic section that occurs from 135 to 550 cm (between 3600 BC and 4 BC). The second group shows the transition zone from ombrotrophic to minerotrophic peat, from 550 to 680 cm (between 4700 BC and 3600 BC), and the third group represents the mean $REE_{UCC}$ values of the minerotrophic section occurs from 680 to 750 cm (between 5300 BC and 4700 BC).

The Misten peat bog has a relatively homogeneous $REE_{UCC}$ composition (Fig. 6). The $REE_{UCC}$ pattern of the three groups shows rather flat spectra with a slight $MREE_{UCC}$ enrichment (Sm, Eu and Gd). The $REE_{UCC}$ pattern in the third group (minerotrophic section) is higher than that shown by the two other groups, which may be explained by dominant local sources (Belgian slate and shale). Both local (Belgian slate and shale) and distal (Sahara aerosol) sources of REE are characterized by a flat pattern (Fig. 6). The Eu anomaly clearly distinguishes minerotrophic against ombrotrophic peat layers (Fig. 4). In minerotrophic peat, there are processes affecting the REE distribution. A large Eu anomaly in the peat $REE_{UCC}$ pattern is occurring in the deepest minerotrophic peat layers and is characteristic of plagioclase minerals (e.g. Pan-African rocks, Cottin et al., 1998). This anomaly in the Misten bog can be explained by the contribution of weathered plagioclase material from local rocks, since the Stavelot Massif lithology, i.e. the geological bedrock, consists of metamorphic rocks, mainly quartzites and phyllites (Ferket et al., 1998) rich in quartz and plagioclase.

### 4.2 Dust source

The REE are immobile in ombrotrophic bog and their concentrations are controlled by atmospheric regional and/or local deposition (Aubert et al., 2006; Kylander et al., 2007; Shotyk et al., 1998, 2001). In general, dust, through its REE abundances and its Nd isotopic signature keeps a fingerprint of its original sources (e.g. Abouchami et al., 1999; Akagi et al., 2002; Aubert et al., 2006; Krachler et al., 2003; Shotyk et al., 2001; Ylirukanen and Lehto, 1995). The origin of the Misten dust can be identified by the sample distribution as shown in diagrams such as $\varepsilon$Nd vs. Sm/Nd and La/Sm vs. La/Yb (Fig. 7a, b). The $\varepsilon$Nd exhibits a large range, from −13 to −5, emphasizing the involvement of contrasting sources during the mid to late Holocene. The diagram $\varepsilon$Nd vs. Sm/Nd (Fig. 7a) shows that the most of the Misten peat samples have an isotopic composition that overlaps that of Sahara aerosols ($\varepsilon$Nd varies between −15 and −11, Abouchami et al., 1999) and that of European loess ($\varepsilon$Nd between −11 and −8, Gallet el al., 1998). The minerotrophic samples (4700–5300 BC) have $\varepsilon$Nd values (from −9 to −5) slightly less negative than those from the ombrotrophic peat samples, suggesting input from local sources (e.g., shale, slate) (Fig. 7a). The erosion of rocks present in the Cambrian–Silurian formations in Belgium (Linnemann et al., 2012) influence the Nd isotopic compositions of sedimentary rocks, as showed by the less negative $\varepsilon$Nd values (−8 to −5, Table 1). The abrupt changes in $\varepsilon$Nd at ∼ 4800 BC ( 2 points with $\varepsilon$Nd around = −6), and ∼ 3100 BC ($\varepsilon$Nd = −5.5) could be due to mantle-derived material like long-range transported volcanic inputs. The first volcanic inputs (4927 ± 98 BC and 4835 ± 79 BC) corresponds to the well-known $\mu$-tephras named Lairg A and Lairg B respectively dated between 4997 and 4902 BC and 4774 and 4677 BC (Lawson et al., 2012). The second point (3200 ± 200 BC) does not correspond to a well-known tephra layer. The local source (Belgium metamorphic rocks) and potential other source (European loess, Sahara aerosol, plagioclase mineral, and Iceland volcanism) are plotted in a La/Sm vs. La/Yb diagram (Fig. 7b). The distribution of the ombrotrophic peat samples (30–4700 BC) suggests a mixing between the local sources (quartzite and phyllade rocks rich in plagioclase) and the regional sources (Sahara aerosol and European loess). The minerotrophic peat samples (4700–5300 BC) are plotted between the La/Sm and La/Yb field defined by for local sources (low in La/Sm and La/Yb ratios, Fig. 7b).

### 4.3 Evolution of dust deposition during the Mid and Late Holocene

Dust deposition in the Misten peat record displays significant variability during the Mid and Late Holocene, with two maxima observed from 3200 to 2800 BC and from 800 to 600 BC. The highest rates of atmospheric dust deposition in Misten peat correspond to cold periods. Since the dust deposition seems to respond with high sensitivity to climate changes, we intend to test the climate imprint in the Misten record during Mid and Late Holocene and especially for the two dust enriched intervals. We integrate dust flux and Nd isotopes to track the climate influence in the Misten peat core. We identify the dominant natural atmospheric supplies by using Nd isotopes composition and interpret the changes of sources as local or global environmental changes. The $\varepsilon$Nd variability is further compared with the testate amoebae assemblages and the humification degree to evaluate the local relative humidity conditions. By using a Suisse peat core, Le Roux et al. (2012) showed that the combination of dust flux and Nd isotope composition may successfully applied to identify the sources of dust and to evidence climate forcing during the Holocene. Local wetness conditions are given by TA assemblages and peat humification degree (Blackford, 2000; Yeloff et al., 2007; Charmaxn et al., 2009). As each individual proxy has its own limitations and problems, it seems clear that a multi-proxy approach is necessary. The different proxies may be partially interdependent but they are all controlled in a more or less direct way to climate. We discuss below the main Holocene stages, i.e. (1) the Atlantic (6000–4000 BC), (2) the Subboreal stage (4000–600 BC) and (3) the Subboreal/Subatlantic transition (600–30 BC).





CPD
9, 2889–2928, 2013

The Misten peat bog (Hautes Fagnes – Belgium)

M. Allan et al.

1. The Atlantic stage corresponds to the warmest period of the Holocene in Greenland (Jonhsen et al., 2001). Peat growth at the Misten site starts at ~5300 BC, and becomes ombrotrophic from 4700 BC. The minerotrophic section (5300–4700) is characterised by a low dust flux (averages of $0.3\,\mathrm{g\,m^{-2}\,yr^{-1}}$). This interval is characterized by wet local conditions attested by the high wet testate amoebae abundance (mean ≈ 49 %), and relatively low humification degree (44–52 %). Similarly, pollen data from the Hautes-Fagnes Plateau show that the studied area was at that time covered by dense mixed mesophilous woodlands (mainly oaks, associated with elms and lime-trees) which were growing up to the edge of and even on peatlands (hazels, alders, ashes and birches), pointing to a wet and warm climate (Damblon, 1994).The $\varepsilon$Nd values vary between −8 and −5 reflecting local deposition and additional volcanic inputs (see above).

   From 4700 to 4000 BC, the dust flux and humification stay relatively constant, with averages of $0.3\,\mathrm{g\,m^{-2}\,yr^{-1}}$ and 50 % respectively. The decrease in percentages of wet testate amoebae to 27 % occurrence, and the better representation of heathlands in pollen diagrams from the area, show slightly drier local environments (Damblon, 1994). For this interval there is no significant change in the dust flux intensity but the relatively dry conditions promote the erosion of local soils confirmed by the $\varepsilon$Nd values (−10 to −9).

2. The Subboreal stage corresponds to the climatic oscillations period, showing a cooling trend in the Northern Hemisphere (Wanner et al., 2008). The Misten dust flux increases compare to the mean value over the Atlantic stage, with pronounced increases during two intervals, from 3200 to 2500 BC and from 800 to 600 BC.

   Between 3200 and 2500 BC, the dust flux reaches values of $2.4\,\mathrm{g\,m^{-2}\,yr^{-1}}$. This interval is characterized by wet local conditions underlined by the high wet testate amoebae content (mean ≈ 60 %) and the low humification degree (mean ≈ 46 %). The humid conditions are in agreement with the vegetal cover changes of the





CPD
9, 2889–2928, 2013

Hautes-Fagnes Plateau deduced from palynology (increase of oak and beech, local increase in hygrophilous and aquatic pollen taxa, Damblon, 1994). Wanner et al. (2011) emphasized a positive humidity anomaly at the scale of Northern Hemisphere between 2800 and 2600 BC. The higher flux records more distal supplies ($\varepsilon$Nd values vary from −9.7 to −11.2, except one sample with $\varepsilon$Nd = −5 reflecting by a volcanic or local source), the local erosion being reduced by the wetter soil conditions, as underlined by a decrease of the humification degree plus a change in the wet testate amoebae content.

Between 2500 and 2000 BC, the dust flux increases to a value $> 1\,\mathrm{g\,m^{-2}\,yr^{-1}}$ at 2100 BC. The general decrease in percentages of wet testate amoebae to 20 % occurrence, and the increase of the humification degree to 52 %, indicates a drier local environment. In this interval $\varepsilon$Nd varies between −9 and −11 reflecting local and regional sources. Then the increasing in dust flux may relate to the important local erosion. By using Spanish speleothems, Martín Chivelet et al. (2011) show that the interval from 2000 to 950 BC is a warm period punctuated by cold events. The glaciers retreat in Europe from 2200–1800 BC (Mayewski et al., 2004) and the lake level minima (Magny, 2004) confirm a warm interval.

Between 1200 and 600 BC, the dust flux increases and reaches the maximum core value ($4.3\,\mathrm{g\,m^{-2}\,yr^{-1}}$). The humification degree decreases to 42 % and wet testate amoebae occurrence declines to ∼ 20 %. The regional pollen data indicate a strong expansion of beech forests at the expense of the mixed oak woodlands, whereas alders and birches developed again near and on wetlands; these changes point to a climatic deterioration with cold and dry conditions, but also to soil degradations (Damblon, 1994). These proxies' variations coincide with a cold event identified by Wanner et al. (2011) between 1300 and 500 BC. The $\varepsilon$Nd displays highly negatives values, reflecting an increased supply from Saharan sources. Damblon (1994) showed that the Human activities appeared in the Hautes -Fagnes Plateau during the late Subboreal, but they remained low and did not seem to have affected local ecological evolution.

3. During the Subboreal/Subatlantic transition (600–30 BC), the dust flux displays highest values (averages of 0.6 $g\,m^{-2}\,yr^{-1}$). At the same time, a low humification degree (35 %) is consistent with cold and dry conditions. An intensification of the human impact is recorded at the same time in the pollen diagrams of the Hautes-Fagnes area (Damblon, 1994) .This period is characterised by influence of human activities related to land use change (regional erosion due to forest clearing and soil cultivation activities) or local and regional climate changes.

### 4.4 Comparison of dust deposition records from peat bogs and ice cores

Among paleoclimate archives, ombrotrophic peat bogs (e.g., Le Roux et al., 2012; Kylander et al., 2007; Marx et al., 2005, 2009; Sapkota et al., 2007; Shotyk et al., 1998) and ice cores (e.g., Delmonte et al., 2004; Lambert et al., 2012; Thompson et al., 1995; Zdanowicz et al., 2000) are unique continental archives which record exclusively the changes in atmospheric deposition of dusts over time. Dust deposition in environments, peat bogs and ice cores, is linked with climatic conditions (e.g. Mahowald et al., 2006; Maher et al., 2010; Thompson, 2006). In order to examine the sensibility of the Misten peat to changes in atmospheric deposition over the mid and late Holocene, we compare the Misten dust record with another European peat bogs (Switzerland, le Roux et al., 2012) and with an ice core collected from Canada (Zdanowicz et al., 2000) (Fig. 9).

The dust flux in the Misten peat ranges from ~0.2 to 4 $g\,m^{-2}\,yr^{-1}$, and reaches its maximum from 3200 to 2800 BC and from 800 to 400 BC. For the Canadian ice core, the dust concentration ranges from ~0.01 to 3 $mg\,kg^{-1}$ and reaches its maximum from 3500 to 3000 BC and from 700 to 200 BC. The warm periods (From 5300 to 3500 and from 2500 to 1200) are linked with a decline in dust flux, and their maximum is associated with a cold event (Lambert et al., 2012). The dust fluxes are 2 to 20 times higher in cold stages defined by Wanner et al. (2012). These two archives show however significant differences in the timing and magnitude of reconstructed dust.

Dust flux reconstructed from the Misten peat core are comparable to results obtained from Swiss peatbogs. The resolution of dust measurement was not the same in the

Misten and Suisse peat cores. By using an ombrotrophic peat at Etang de la Gruere in Switzerland, Le Roux et al. (2012) showed that the dust flux varies between 0.1 and 5 $g\,m^{-2}\,yr^{-1}$ from 6000 to 20 BC. The dust flux measured in Misten peat varies within a same range, from 0.1 to 4.5 $g\,m^{-2}\,yr^{-1}$ from 5300 to 30 BC. The dust fluxes in both peat cores was at a minimum (< 1 $g\,m^{-2}\,yr^{-1}$) from 5500 to 3500 BC, except at 4000 BC when dust fluxes measured in the Suisse peat reached 2.5 $g\,m^{-2}\,yr^{-1}$ corresponding an unknown event. The dust deposition increased markedly between 3500 and 1200 BC and the maximum occurred at 1300 BC as shown in Fig. 9 (Le Roux et al., 2012). These changes were linked to first signs of forest clearing and the beginning of plant cultivation (Shotyk et al., 2002). A significant contribution of dust starts in the Suisse peat after 4000 BC, which is in agreement with the Sahara desertification. This timing of Sahara expansion, between 6000 BC and 3500 BC, is supported by paleoenvironmental data from the west African Atlantic coast, wwhen the Saharan vegetation cover decreased from 0.9 to 0 % and the terrigenous material increased from 40 to 52 % (Claussen et al., 1999; deMenocal et al., 2000).

In the Misten peat, dust fluxes oscillate between 3500 and 1200 BC and reaches a maximum (2.5 $g\,m^{-2}\,yr^{-1}$) at 3000 BC. Its timing corresponds to a cold event described by Wanner et al. (2011). From 500 to 20 BC, dust flux measured in Swiss peat core (Le Roux et al., 2012) ranges between 2 and 3 $g\,m^{-2}\,yr^{-1}$; up to 5 × higher that that measured in the Misten peat core (dust flux ranges from 0.2 to 0.8 $g\,m^{-2}\,yr^{-1}$). This difference in dust flux would be an indication for increased human activities (open pasture, agriculture and mining activities). Anthropogenic effects explaining the maximum in the Swiss peat bog does not seem to have an important effect during this period in the Misten core. Sjogren (2006) showed that the open pastures are started around Etang de la Gruère bog during the first centuries BC as shown by peat studies, but it only started around Misten peatland after AD 1100 (De Vleeschouwer et al., 2012).

Our study, by using dust deposition and Nd isotopes, showed that Saharan dust has played an essential role in dust loading over Europe both on a long term basis but also during abrupt events such as from 3200 to 2800 BC and from 800 to 600 BC.

## 5 Conclusions

Elemental concentrations and Nd isotopes analysed in a $\sim 6$ m peat core collected from the Hautes-Fagnes Plateau (Southern Belgium), allow to identify dust sources. Humification and testate amoebae have been used to reconstruct the climatic conditions during the mid and late Holocene. The clear correlation between REE and conservative elements concentrations (Ti, Al, Zr) in the Misten peat core confirm that the complete atmospheric REE input is preserved in the peat bog. The general agreement between the dust flux and the paleo-hydrological proxies (humification and testate amoebae) confirms the increase in dust deposition in peat during cold periods and therefore confirms the direct climatic influence on dust input. To identify the dust sources, we compared the Nd isotopic ratios and REE ratios of Misten peat with those of different potential local and regional sources. The $\varepsilon$Nd range from $-14$ to $-5$, reflecting a diversity of sources during mid and late Holocene, with large supplies from distal (Sahara), regional (European loess), local aerosols ad distal volcanic particles from Iceland. After 4000 BC, sources were restricted to the Saharan and European aerosols, indicating locally wetter conditions. The average dust flux over the 5500 yr represented by the core was 0.5 $\mathrm{g\,m^{-2}\,yr^{-1}}$, while dust flux reached as high as $> 2\,\mathrm{g\,m^{-2}\,yr^{-1}}$ between 3200–2800 BC and around 800 BC. Comparison between the Misten record and a peat record from Switzerland show that humans influenced regionally the dust cycle earlier in Switzerland than in the hostile environment of Plateau des Hautes Fagnes where the Misten bog is located.

*Acknowledgements.* This study was funded by the Walloon Region and the FNRS. M. Allan received funding through a Ph.D. grant from the government of Syria.





CPD
9, 2889–2928, 2013
The Misten peat bog (Hautes Fagnes – Belgium)
M. Allan et al.

## References

Abouchami, W., Galer, S. J. G., and Koschinsky, A.: Pb and Nd isotopes in NE Atlantic Fe–Mn crusts: proxies for trace metal paleosources and paleocean circulation, Geochim. Cosmochim. Ac., 63, 1489–1505, 1999.

Akagi, T., Feng-Fu, F., and Yabuki, S.: Absence of Ce anomaly in the REE patterns of peat moss and peat grass in the Ozegahara peatland, Geochem. J., 36, 113–118, 2002.

Ali, A. and Srinivasan, G.: Precise thermal ionization mass spectrometric measurements of $^{142}Nd/^{144}Nd$ and $^{143}Nd/^{144}Nd$ isotopic ratios of Nd separated from geological standards by chromatographic methods, Int. J. Mass. Spectrom., 299, 27–34, 2011.

André, L., Deutsch, S., and Hertogen, J.: Trace-element and Nd isotopes in shales as indexes of provenance and crustal growth: the early Paleozoic from the Brabant Massif (Belgium), Chem. Geol., 57, 101–115, 1986.

Aubert, D., Le Roux, G., Krachler, M., Cheburkin, A., Kober, B., Shotyk, W., and Stille, P.: Origin and fluxes of atmospheric REE entering an ombrotrophic peat bog in Black Forest (SW Germany): evidence from snow, lichens and mosses, Geochim. Cosmochim. Ac., 70, 2815–2826, 2006.

Bar-Matthews, M., Ayalon, A., Kaufman, A., and Wasserburg, G. J.: The eastern Mediterranean paleoclimate as a reflection of regional events: Soreq Cave, Israel, Earth Planet. Sc. Lett., 166, 85–95, 1999.

Belokopytov, I. E. and Veresnevich, V. V.: Giktorf's peat borers, Torfânaâ promyslennost, 8, 9–10, 1955.

Blaauw, M. and Christen, J. A.: Flexible paleoclimate age-depth models using an autoregressive gamma process, Bayesian Analysis, 6, 457–474, 2011.

Blaauw, M., van Geel, B., and van der Plicht, J.: Solar forcing of climate change during the mid-Holocene: indications from raised bogs in the Netherlands, Holocene, 14, 34–44, 2004.

Blackford, J. J.: Palaeoclimatic records from peat bogs, Trends Ecol. Evol., 15, 193–198, 2000.

Bond, G., Kromer, B., Beer, J., Muscheler, R., Evans, M. N., Showers, W., Hoffmann, S., Lotti-Bond, R., Hajdas, I., and Bonani, G.: Persistent solar influence on North Atlantic climate during the Holocene, Science, 294, 2130–2136, 2001.

Booth, R. K., Jackson, S. T., and Gray, C. E. D.: Paleoecology and high-resolution paleohydrology of a kettle peatland in upper Michigan, Quaternary Res., 61, 1–13, 2004.

Booth, R. K., Lamentowicz, M., and Charman, D. J.: Preparation and analysis of testate amoebae in peatland palaeoenvironmental studies, Mires and Peat, 7, 1–7, 2010.
Bronk, R. C.: Bayesian analysis of radiocarbon dates, Radiocarbon, 51, 337–360, 2009.
Chambers, F. M., Booth, R. K., De Vleeschouwer, F., Lamentowicz, M., Le Roux, G., Mauquoy, D., Nichols, J. E., and van Geel, B.: Development and refinement of proxy-climate indicators from peats, Quatern. Int., 28, 1811–1819, doi:10.1016/j.quaint.2011.04.039, 2011.
Charman, D. J., Hendon, D., and Woodland, W.: The Identification of Peatland Testate Amoebae, Quaternary Research Association Technical Guide no. 9, Quaternary Research Association, London, United Kingdom, 2000.
Charman, D. J., Barber, K. E., Blaauw, M., Langdon, P. G., Mauquoy, D., Daley, T. J., Hughes, P. D. M., and Karofeld, E.: Climate drivers for peatland palaeoclimate records, Quaternary Sci. Rev., 28, 1811–1818, 2009.
Chauvel, C. and Blichert-Toft, J.: A hafnium isotope and trace element perspective on melting of the depleted mantle, Earth Planet. Sc. Lett., 190, 137–151, 2001.
Claussen, M., Kubatzki, C., Brovkin, V., Ganopolski, A., Hoelzmann, P., and Pachur, H. J.: Simulation of an abrupt change in Saharan vegetation in the mid-Holocene, Geophys. Res. Lett., 26, 2037–2040, doi:10.1029/1999GL900494, 1999.
Cottin, J. Y., Lorand, J. P., Agrinier, P., Bodinier, J. L., and Lieegeois, J. P.: Isotopic (O, Sr, Nd) and trace element geochemistry of the Laouni layered intrusions (Pan-African belt, Hoggar, Algeria): evidence for post-collisional tholeiitic magmas variably contaminated by continental crust, Lithos, 45, 197–222, 1998.
Damblon, F.: Les dépôts tourbeux et l'histoire de la végétation sur le plateau des Hautes-Fagnes (Belgique), Ann. Soc. Géol. Belgique, 117, 259–276, 1994.
Davis, B. A. S. and Brewer, S.: Orbital forcing and the role of the Latitudinal Temperature/Isolation Gradient, Clim. Dynam., 32, 143–165, 2009.
Davis, B. A. S., Brewer, S., Stevenson, A. C., Guiot, J., Allen, J., Almqvist-Jacobson, H., Ammann, B., Andreev, A. A., Argant, J., Atanassova, J., Balwierz, Z., Barnosky, C. D., Bartley, D. D., De Beaulieu, J. L., Beckett, S. C., Behre, K. E., Bennett, K. D., Berglund, B. E. B., Beug, H.-J, Bezusko, L., Binka, K., Birks, H. H., Birks, H. J. B., Björck, S., Bliakhartchouk, T., Bogdel, I., Bonatti, E., Bottema, S., Bozilova, E. D. B., Bradshaw, R., Brown, A. P., Brugiapaglia, E., Carrion, J., Chernavskaya, M., Clerc, J., Clet, M., Coûteaux, M., Craig, A. J., Cserny, T., Cwynar, L. C., Dambach, K., De Valk, E. J., Digerfeldt, G., Diot, M. F., Eastwood,





CPD
9, 2889–2928, 2013

The Misten peat bog (Hautes Fagnes – Belgium)

M. Allan et al.

W., Elina, G., Filimonova, L., Filipovitch, L., Gaillard-Lemdhal, M. J., Gauthier, A., Göransson, H., Guenet, P., Gunova, V., Hall, V. A. H., Harmata, K., Hicks, S., Huckerby, E., Huntley, B., Huttunen, A., Hyvärinen, H., Ilves, E., Jacobson, G. L., Jahns, S., Jankovská, V., Jóhansen, J., Kabailiene, M., Kelly, M. G., Khomutova, V. I., Königsson, L. K., Kremenetski, C., Kremenetskii, K. V., Krisai, I., Krisai, R., Kvavadze, E., Lamb, H., Lazarova, M. A., Litt, T., Lotter, A. F., Lowe, J. J., Magyari, E., Makohonienko, M., Mamakowa, K., Mangerud, J., Mariscal, B., Markgraf, V., McKeever, Mitchell, F. J. G., Munuera, M., Nicol-Pichard, S., Noryskiewicz, B., Odgaard, B. V., Panova, N. K., Pantaleon-Cano, J., Paus, A. A., Pavel, T., Peglar, S. M., Penalba, M. C., Pennington, W., and Perez-Obiol, R: The temperature of Europe during the Holocene reconstructed from pollen data, Quaternary Sci. Rev., 22, 1701–1716, 2003.

DeMenocal, P., Ortiz, J., Guilderson, T., Adkins, J., Sarnthein, M., Baker, L., and Yarusinsky, M.: Abrupt onset and termination of the African humid period: rapid climate responses to gradual insolation forcing, Quaternary Sci. Rev., 19, 347–361, doi:10.1016/S0277-3791(99)00081-5, 2000.

De Paolo, D. J. and Wasserburg, G. J.: Nd isotope variations and netrogenetic models, Geoohvs. Res. Let. Washington, 3, 6017–6040, 1976.

De Vleeschouwer, F., Gérard, L., Goormaghtigh, C., Mattielli, N., Le Roux, G., and Fagel, N.: Atmospheric lead and heavy metal pollution records from a Belgian peat bog spanning the last two millennia: human impact on a regional to global scale, Sci. Total Environ., 377, 282–295, 2007.

De Vleeschouwer, F., Luthers, C., Mauquoy, D., Wastiaux, C., Le Roux, G., Moschen, R., Pawlyta, J., Pazdur, A., Sikorski, J., and Piotrowska, N.: Multiproxy paleoenvironmental study in the Misten bog (East Belgium) during the last millennium, Quatern. Int., 268, 44–57, 2012.

Delmonte, B., Petit, J. R., and Maggi, V.: Glacial to Holocene implications of the new 27 000-year dust record from the EPICA Dome C (East Antarctica) ice core, Clim. Dynam., 18, 647–660, 2002.

Delmonte, B., Basile-Doelsch, I., Petit, J. R., Maggi, V., Revel-Rolland, M., Michard, A., Jagoutz, E., and Grousset, F.: Comparing the EPICA and Vostok dust records during the last 220 000 years: stratographical correlation and origin in glacial periods, Earth Sci. Rev., 66, 63–87, 2004.





CPD
9, 2889–2928, 2013

The Misten peat bog (Hautes Fagnes – Belgium)

M. Allan et al.

Fagel, N., Innocent, C., Stevenson, R., and Hillaire-Marcel, C.: Deep circulation changes in the Labrador Sea since the Last Glacial Maximum: new constraints from Sm–Nd data on sediments, Paleoceanography, 14, 0883–8305, 1999.
Ferket, H., Muchez, P., Schroyen, K., and Sintubin, M.: Metamorphism in the Stavelot-Venn Massif: a study of quartz veins in the basal devonian conglomerates (Lochkovian), Aardkundige Mededelingen, 9, 7–16, 1998.
Frumkin, A. and Stein, M.: The Sahara–East Mediterranean dust and climate connection revealed by strontium and uranium isotopes in a Jerusalem speleothem, Earth Planet. Sc. Lett., 217, 451–464, 2004.
Gabrielli, P., Wegner, A., Petit, J. R., Delmonte, B., De Deckker, P., Gaspari, V., Fischer, H., Ruth, U., Kriews, M., Boutron, C., Cescon, P., and Barbante, C.: A major glacial-interglacial change in aeolian dust composition inferred from Rare Earth Elements in Antarctic ice, Quaternary Sci. Rev., 29, 265–273, 2010.
Gallet, S., Jahn, B., Lanoe, B. V. V., Dia, A., and Rossello, E.: Loess geochemistry and its implications for particle origin and composition of the upper continental crust, Earth Planet. Sc. Lett., 156, 157–172, 1998.
Givelet, N., Le Roux G., Cheburkin, A., Chen, B., Frank, J., Goodsite, M. E., Kempter, H., Krachler, M., Noernberg, T., Rausch, N., Rheinberger, S., Roos-Barraclough, F., Sapkota, A., Scholz, C., and Shotyk, W.: Suggested protocol for collecting, handling and preparing peat cores and peat samples for physical, chemical, mineralogical and isotopic analyses, J. Environ. Monitor., 6, 481–492, 2004.
Goossens, D.: Dry aeolian dust accumulation in rocky deserts: a medium-term field experiment based on short-term wind tunnel simulations, Earth Surf. Processes, 25, 41–57, 2000.
Goudie, A. S.: The global distribution of dust storms, Ann. Arid Zone, 40, 1–12, 2001.
Goudie, A. S. and Middleton, N. J.: Desert Dust in the Global System, Springer, London, United Kingdom, 2006.
Grousset, F. E. and Biscaye, P. E.: Continental aerosols, isotopic fingerprints of sources and atmospheric transport: a review, Chem. Geol., 222, 149–167, 2005.
Grousset, F. E., Ginoux, P., Bory, A., and Biscaye, P. E.: Case study of a Chinese dust plume reaching the French Alps, Geophys. Res. Lett., 30, 1277, doi:10.1029/2002GL016833, 2003.
Handley, H. K., Turner, S., Macpherson, C. G., Gertisser, R., and Davidson, J. P.: Hf–Nd isotope and trace element constraints on subduction inputs at island arcs: limitations of Hf anomalies as sediment input indicators, Earth Planet. Sc. Lett., 304, 212–223, 2011.





CPD
9, 2889–2928, 2013

Heikkila, M. and Seppa, H.: A 11 000 yr palaeotemperature reconstruction from the southern boreal zone in Finland, Quaternary Sci. Rev., 22, 541–554, 2003.

Jonhsen, S. J., Jensen, D. D., Gundestrup, N., Steffensen, J. P., Clausen, H. B., Miller, H., Masson-Delmotte, V., Sveinbjörnsdottir, A. E., and White, J.: Oxygen isotope and palaeotemperature records from six Greenland ice core stations: Camp Century, Dye 3, GRIP, GISP2, Renland and NorthGRIP, J. Quaternary Sci., 16, 299–307, 2001.

Kamanov, G. D., Brenner, M., and Tucker, J. L.: Anthropogenic versus natural control on trace element and Sr–Nd–Pb isotiope stratigraphy in peat sediments of southeast Florida (USA), ~1500 AD to present, Geochim. Cosmochim. Ac., 73, 3549–3567, 2009.

Kylander, M. E., Muller, J., Wust, R. A. J., Gallagher, K., GarciaSanchez, R., Coles, B. J., and Weiss, D. J.: Rare earth elementand Pb isotope variations in a 52 kyr peat core from Lynch's Crater (NE Queensland, Australia): proxy development and application to paleoclimate in the Southern Hemisphere, Geochim. Cosmochim. Ac., 71, 942–60, 2007.

Lambert, F., Bigler, M., Steffensen, J. P., Hutterli, M., and Fischer, H.: Centennial mineral dust variability in high-resolution ice core data from Dome C, Antarctica, Clim. Past, 8, 609–623, doi:10.5194/cp-8-609-2012, 2012.

Lamentowicz, M., Obremska, M., and Mitchell, E. A. D.: Autogenic succession, land-use change, and climatic influences on the Holocene development of a kettle hole mire in Northern Poland, Rev. Palaeobot. Palyno., 151, 21–40, 2008.

Larocque, I. and Bigler, C.: Similarities and discrepancies between chironomid- and diatom-inferred temperature reconstructions through the Holocene at Lake 850, northern Sweden, Quatern. Int., 122, 109–121, 2004.

Lawrence, C. R. and Neff, J. C.: The contemporary physical and chemical flux of Aeolian dust: a synthesis of direct measurements of dust deposition, Chem. Geol., 267, 46–63, 2009.

Lawson, I. T., Swindles, G. T., Plunkett, G., and Greenberg, D.: The spatial distribution of Holocene cryptotephras in north-west Europe since 7 ka: implications for understanding ash fall events from Icelandic eruptions, Quarternary Sci. Rev., 41, 57–66, 2012.

Le Roux, G., Fagel, N., De Vleeschouwe, F., Krachler, M., Debaille, V., Stille, P., Mattelli, N., Van der Knaap, W. O., Van Leeuwen, J. F. N., and Shotyk, W.: Volcano- and climate-driven changes in atmospheric dust sources and fluxes since the Late Glacial in Central Europe, Geology, 40, 335–338, 2012.

Linnemann, U., Herbosch, A., Liégeois, J.-P., Pin, C., Gärtner, A., and Hofmann, M.: The Cambrian to Devon ian odyssey of the Brabant Massif within Avalonia: a review with the new

zircon ages, geochemistry, Sm–Nd isotopes, stratigraphy and palaeogeography, Earth Sci. Rev., 112, 126–154, 2012.
Magny, M.: Holocene climatic variability as reflected by mid-European lake-level fluctuations, and its probable impact on prehistoric human settlements, Quatern. Int., 113, 65–80, 2004.
Magny, M., Leuzinger, U., Bortenschlager, S., and Haas, J. N.: Tripartite climate reversal in central Europe 5600–5300 years ago, Quaternary Res., 65, 3–19, 2006.
Mahowald, N. M., Muhs, D. R., Levis, S., Rasch, P. J., Yoshioka, M., Zender, C. S., and Luo, C.: Change in atmospheric mineral aerosols in response to climate: last Glacial period, preindustrial, modern, and doubled carbon dioxide climates, J. Geophys. Res., 111, D10202, doi:10.1029/2005JD006653, 2006.
Martín-Chivelet, J., Muñoz-García, M. B., Edwards, R. L., Turrero, M. J., and Ortega, A. I.: Northern Spain 4000 year stalagmite $d^{13}C$ and temperature reconstruction, Global Planet. Change, 77, 1–12, 2011.
Marx, S. K., Kamber, B. S., and McGowan, H. A.: Provenance of long travelled dust determined with ultra-trace-element composition: a pilot study with samples from New Zealand glaciers, Earth Surf. Proc. Land., 30, 699–716, 2005.
Marx, S. K., McGowan, H. A., and Kamber, B. S.: Long-range dust transport from eastern Australia: a proxy for Holocene aridity and ENSO-induced climate variability, Earth Planet. Sc. Lett., 282, 167–177, 2009.
Marx, S. K., Kamber, B. S., McGowan, H. A., and Denholm, J.: Holocene dust deposition rates in Australia's Murray–Darling Basin, record the interplay between aridity, position of the mid-latitude westerlies, Quarternary Sci. Rev., 30, 3290–3305, 2011.
Mayewski, P. A., Rohling, E. E., Stager, J. C., Karlen, W., Maasch, K. A., Meeker, L. D., Meyerson, E. A., Gasse, F., van Kreveld, S., Holmgren, K., Lee-Thorp, J., Rosqvist, G. Rack, F., Staubwasser, M., Schneider, R. R., and and Steig, E. J.: Holocene climate variability, Quaternary Res., 62, 243–255, 2004.
Meskhidze, N., Chameides, W. L., Nenes, A., and and Chen, G.: Iron mobilization in mineral dust: can anthropogenic $SO_2$ emissions affect ocean productivity?, Geophys. Res. Lett., 30, 2085, doi:10.1029/2003GL018035, 2003.
Moreno, T., Castillo, S., Alastuey, A., Cuevas, E., Herrmann, L., Mounkaila, M., Elvira, J., and Gibbons, W.: Geochemical variations in aeolian mineral particles from the Sahara–Sahel dust corridor, Chemosphere, 65, 261–270, 2006.

Müller, B., Höhne, N., and Ellermann, C.: Differentiating (Historic) Responsibilities for Climate Change, Oxford Institute for Energy Studies (OIES), University of Oxford, Oxford, Royaume-Un., 2007.
Niggemann, S., Mangini, A., Richter, D. K., and Wurth, G.: A paleoclimate record of the last 17 600 years in stalagmites from the B7 cave, Sauerland, Germany, Quaternary Sci. Rev., 22, 555–567, 2003.
Payne, R. J.: Can testate amoeba-based palaeohydrology be extended to fens?, J. Quaternary Sci., 26, 15–27, 2011.
Payne, R. J. and Mitchell, E. A. D.: How many is enough? Determining optimal count totals for ecological and palaeoecological studies of testate amoebae, J. Paleolimnol., 42, 483–495, 2009.
Piotrowska, N.: Status report of AMS sample preparation laboratory at GADAM Centre, Gliwice, Poland, Nucl. Instrum. Meth. B, 294, 176–181, 2013.
Piotrowska, N., Blaauw, M., Mauquoy, D., and Chambers, F. M.: Constructing deposition chronologies for peat deposits using radiocarbon dating, Mires and Peat, 7, 10, 2011.
Plunkett, G. and Swindles, G. T.: Determining the Sun's influence on Late Glacial and Holocene climates: a focus on climate response to centennial-scale solar forcing at 2800 cal. BP, Quaternary Sci. Rev., 27, 175–184, 2008.
Reimer, P. J., Baillie, M. G. L., Bard, E., Bayliss, A., Beck, J. W., Blackwell, P. G., Bronk Ramsey, C., Buck, C. E., Burr, G., Edwards, R. L., Friedrich, M., Grootes, P. M., Guilderson, T. P., Hajdas, I., Heaton, T. J., Hogg, A. G., Hughen, K. A., Kaiser, K. F., Kromer, B., McCormac, F. G., Manning, S. W., Reimer, R. W., Richards, D. A., Southon, J., Turney, C. S. M., van der Plicht, J., and Weyhenmeyer, C.: IntCal09 and Marine09 radiocarbon age calibration curves, 0–50 000 years cal BP, Radiocarbon, 5, 1111–1150, 2009.
Roos-Barraclough, F., Martinez-Cortizas, A., Garcla-Rodeja, E., and Shotyk, W.: A 14 500 year record of the accumulation of atmospheric mercury in peat: volcanic signals, anthropogenic influences and a correlation to bromine accumulation, Earth Planet. Sc. Lett., 202, 435–451, 2002.
Sapkota, A.: Mineralogical, Chemical, and Isotopic (Sr, Pb) Composition of Atmospheric Mineral Dusts in an Ombrotrophic Peat Bog, Southern South America, PhD Thesis, Ruprecht-Karls-Universität, Heidelberg, Germany, 2006.
Sapkota, A., Cheburkin, A. K., Bonani, G., and Shotyk, W.: Six millenia of atmospheric dust deposition in southern South America (Isla Navarino, Chile), Holocene, 17, 561–572, 2007.

Shotyk, W.: Peat bog archives of atmospheric metal deposition: geochemical evaluation of peat profiles, natural variations in metal concentrations, and metal enrichment, Environ. Rev., 4, 149–183, 1996.

Shotyk, W., Weiss, D., Appleby, P. G., Cheburkin, A. K., Frei, R., Gloor, M., Kramers, J. D., Reese, S., and van der Knaap, W. O.: History of atmospheric lead deposition since 12 370 $^{14}$C yr BP recorded in a peat bog profile, Jura Mountains, Switzerland, Science, 281, 1635–1640, 1998.

Shotyk, W., Weiss, D., Kramers, J. D., Frei, R., Cheburkin, A. K., Gloor, M., and Reese, S.: Geochemistry of the peat bog at Etang de la Gruère, Jura Mountains, Switzerland, and its record of atmospheric Pb and lithogenic trace metals (Sc, Ti, Y, Zr, and REE) since 12 370 $^{14}$C yr BP, Geochim. Cosmochim. Ac., 65, 2337–2360, 2001.

Shotyk, W., Krachler M., Martinez-Cortizas, A., Cheburkin, A. K., and Emons, H.: A peat bog record of natural, pre-anthropogenic enrichments of trace elements in atmospheric aerosols since 12 370 $^{14}$C yr BP, and their variation with Holocene climate change, Earth Planet. Sc. Lett., 199, 21–37, 2002.

Sirocko, F., Dietrich, S., Veres, D., Grootes, P. M., Schaber-Mohr, K., Seelos, K., Nadeau, M. J., Kromer, B., Leo Rothacker, L., Rohner, M., Krbetschek, M., Appleby, P. G., Hambach, U., Rolf, C., Sudo, M., and Grim S.: Multi-proxy dating of Holocene maar lakes and Pleistocene dry maar sediments in the Eifel, Germany, Quaternary Sci. Rev., 62, 56–76, 2013.

Sillasoo, U., Mauquoy, D., Blundell, A., Charman, D., Blaauw, M., Daniell, J. R. G., Toms, P., Newberry, J., Chambers, F. M., and Karofeld, E.: Peat multi-proxy data from Mannikjarve bog as indicators of late Holocene climate changes in Estonia, Boreas, 36, 20–37, 2007.

Sjogren, P.: The development of pasture woodland in the southwest Swiss Jura Mountains over 2000 years, based on three adjacent peat profiles, Holocene, 16, 210–223, 2006.

Speranza, A., van Geel, B., and van der Plicht, J.: Evidence for solar forcing of climate change at ca. 850 cal BC from a Czech peatsequence, Global Planet. Change, 35, 51–65, 2002.

Taylor, S. R. and McLennan, S. M.:The Continental Crust: its Composition and Evolution, Blackwell, Oxford, 1985.

Thompson, L. G., Mosley-Thompson, E., Davis, M. Lin, P. N., Henderson, K. A., Cole-Dai, J., Bolzan, J. F., and Liu, K. B.: Late glacial stage and Holocene tropical ice core records from Huascaran, Peru, Science, 269, 46–50, 1995.

Thompson, L. G., Mosley-Thompson, E., Davis, M. E., Henderson, K. A., Brecher, H. H., Zagorodnov, V. S., Mashiotta, T. A., Lin, P.-N., Mikhalenko, V. N., Hardy, D. R., Beer, J., Ice core records: evidence of Holocene climate change in tropical Africa, Science, 298, 589–593, 2000.

Thompson, L. G., Mosley-Thompson, E., Davis, M. E., Lin, P. N., Henderson, K., and Mashiotta, T. A.: Tropical glacier and ice core evidence of climate change on annual to millennial timescales, Climatic Change, 59, 137–155, 2003.

Tegen, I., Harrison, S. P., Kohfeld, K. E., Engelstaedter, S., and Werner, M.: Emission of soil dust aerosol: anthropogenic contribution and future changes, Geochim. Cosmochim. Ac., 66, A766–A766, 2002.

Tegen, I., Werner, M., Harrison, S. P., and Kohfeld, K. E.: Relative importance of climate and land use in determining present and future global soil dust emission, Geophys. Res. Lett., 31, L05105, doi:10.1029/2003GL019216, 2004.

van Geel, B., Buurman, J., and Waterbolk, H. T.: Archaeological and palaeoecological indications for an abrupt climate change in the Netherlands and evidence for climatological teleconnections around 2650 BP, J. Quaternary Sci., 11, 451–460, 1996.

Verheyden, S., Genty, D., Deflandre, G., Quinif, Y., and Keppens, E.: Monitoring climatological, hydrological and geochemical parameters in the Père Noël Cave (Belgium): implication for the interpretation of speleothem isotopic and geochemical time-series, Int. J. Speleol., 37, 221–234, 2008.

Warner, B. G., Asada, T., and Quinn, N. P.: Seasonal influences on the ecology of testate amoebae (protozoa) in a small Sphagnum peatland in Southern Ontario, Cananda, Microbial Ecol., 54, 91–100, 2007.

Wanner, H., Beer, J., Butikofer, J., Crowley, T., Cubasch, U., Fluckiger, J., Goosse, H., Grosjean, M., Joos, F., Kaplan, J. O., Kuttel, M., Muller, S., Pentice, C., Solomina, O., Stocker, T., Tarasov, P., Wagner, M., and Widmann, M.: Mid to late Holocene climate change – an overview, Quaternary Sci. Rev., 27, 1791–1828, 2008.

Wanner, H., Solomina, O., Grosjean, M., Ritz, S. P., and Jetel, M.: Structure and origin of Holocene cold events, Quaternary Sci. Rev., 30, 3109–3123, 2011.

Wardenaar, E.: A new hand tool for cutting peat profiles, Revue Canadienne de Botanique, 65, 1771–1772, 1987.

Wastiaux, C. and Schumacker, R.: Topographie de Surface et de Subsurface des Zones Tourbeuses des Réserves Naturelles Domaniales des Hautes-Fagnes, Rapport de Synthèse, Convention C60 entre l'Université de Liège et le Ministère de la Région Wallonne (D.G.R.N.E.), rapport inédit, 52 pp., 2003.

Yeloff, D., Charman, D., van Geel, B., and Mauquoy, D.: Reconstruction of hydrology, vegetation and past climate change in bogs using fungal microfossils, Rev. Palaeobot. Palyno., 146, 102–145, 2007.
Ylirukanen, I. and Lehto, S.: The occurrence of rare earth elements in some Finnish mires, Bull. Geol. Soc. Finl., 5, 27–38, 1995.
Zdanowicz, C. M., Zielinski, G. A., Wake, C., Fisher, D. A., and Koerner, R. M.: A Holocene record of atmospheric dust deposition on the Penny Ice Cap, Baffin Island, Canada, Quaternary Res., 53, 62–69, 2000.

**Table 1.** Sm–Nd analytical results of the samples from the Misten peat.

| Sample | Depth (cm) | Min age AD/BC | Max age BC | Mean age BC | $^{143}$Nd/$^{144}$Nd | 2se | εNd |
|---|---|---|---|---|---|---|---|
| 129 | 134 | 8 | −147 | −20 | 0.5120669 | 0.00001 | −11.1 |
| 130 | 135 | −1 | −166 | −37 | 0.5120460 | 0.00002 | −11.5 |
| 132 | 139 | −61 | −196 | −117 | 0.5121101 | 0.00003 | −10.3 |
| 158 | 146 | −97 | −257 | −236 | 0.5120610 | 0.00002 | −11.3 |
| 142 | 170 | −242 | −407 | −392 | 0.5120628 | 0.00002 | −11.2 |
| 169 | 185 | −327 | −497 | −454 | 0.5120180 | 0.00001 | −12.1 |
| 172 | 189 | −353 | −523 | −464 | 0.5120856 | 0.00001 | −10.8 |
| 178 | 198 | −403 | −588 | −544 | 0.5120364 | 0.00001 | −11.7 |
| 182 | 204 | −419 | −609 | −574 | 0.5121009 | 0.00001 | −10.5 |
| 196 | 225 | −568 | −698 | −682 | 0.5120130 | 0.00001 | −12.2 |
| 203 | 230 | −609 | −709 | −696 | 0.5119776 | 0.00001 | −12.9 |
| 209 | 239 | −659 | −744 | −737 | 0.5120455 | 0.00001 | −11.6 |
| 221 | 257 | −771 | −921 | −826 | 0.5120137 | 0.00001 | −12.2 |
| 224 | 261 | −794 | −1009 | −864 | 0.5120627 | 0.00001 | −11.2 |
| 239 | 278 | −985 | −1220 | −1047 | 0.5120992 | 0.00001 | −10.5 |
| 245 | 288 | −1146 | −1296 | −1159 | 0.5120382 | 0.00001 | −11.7 |
| 248 | 293 | −1182 | −1372 | −1222 | 0.5121002 | 0.00001 | −10.5 |
| 257 | 307 | −1299 | −1559 | −1342 | 0.5120936 | 0.00001 | −10.6 |
| 269 | 321 | −1443 | −1683 | −1545 | 0.5121232 | 0.00001 | −10.0 |
| 297 | 364 | −1843 | −2058 | −1934 | 0.5121395 | 0.00002 | −9.7 |
| 311 | 380 | −1941 | −2181 | −2019 | 0.5120793 | 0.00001 | −10.9 |
| 320 | 393 | −2042 | −2257 | −2106 | 0.5120760 | 0.00002 | −11.0 |
| 329 | 407 | −2139 | −2324 | −2173 | 0.5120777 | 0.00001 | −10.9 |
| 335 | 410 | −2161 | −2346 | −2198 | 0.5121256 | 0.00002 | −10.0 |
| 346 | 426 | −2303 | −2553 | −2386 | 0.5121601 | 0.02901 | −9.3 |
| 347 | 428 | −2334 | −2574 | −2424 | 0.5114899 | 0.00002 | −11.0 |
| 348 | 429 | −2340 | −2590 | −2443 | 0.5120902 | 0.02675 | −10.7 |
| 353 | 437 | −2401 | −2671 | −2533 | 0.5121396 | 0.00004 | −9.7 |
| 362 | 450 | −2499 | −2799 | −2669 | 0.5121375 | 0.00001 | −9.8 |
| 364 | 454 | −2543 | −2838 | −2712 | 0.5120951 | 0.00001 | −10.6 |
| 372 | 461 | −2654 | −2894 | −2803 | 0.5120659 | 0.00001 | −11.2 |
| 377 | 468 | −2740 | −2970 | −2866 | 0.5121012 | 0.00003 | −10.5 |
| 383 | 477 | −2885 | −3030 | −2906 | 0.5121426 | 0.00001 | −9.7 |
| 392 | 491 | −2978 | −3213 | −3004 | 0.5121105 | 0.00001 | −10.3 |
| 401 | 500 | −3041 | −3316 | −3104 | 0.5123538 | 0.00005 | −5.5 |
| 404 | 504 | −3076 | −3336 | −3159 | 0.5121058 | 0.00001 | −10.4 |
| 410 | 513 | −3159 | −3439 | −3259 | 0.5121088 | 0.00001 | −10.3 |
| 413 | 518 | −3200 | −3480 | −3310 | 0.5120836 | 0.00001 | −10.8 |
| 428 | 540 | −3390 | −3690 | −3566 | 0.5120002 | 0.00001 | −12.4 |
| 437 | 549 | −3478 | −3763 | −3620 | 0.5121309 | 0.00001 | −9.9 |
| 443 | 558 | −3591 | −3846 | −3736 | 0.5121284 | 0.00001 | −9.9 |
| 449 | 567 | −3727 | −3902 | −3799 | 0.5121436 | 0.00001 | −9.6 |
| 455 | 576 | −3788 | −3983 | −3857 | 0.5121391 | 0.00002 | −9.7 |
| 461 | 585 | −3846 | −4031 | −3918 | 0.5122329 | 0.00002 | −7.9 |
| 464 | 588 | −3869 | −4049 | −3954 | 0.5121023 | 0.00001 | −10.5 |
| 476 | 603 | −3978 | −4173 | −4029 | 0.5121120 | 0.00001 | −10.3 |
| 484 | 615 | −4050 | −4280 | −4132 | 0.5121573 | 0.00001 | −9.4 |
| 494 | 630 | −4161 | −4391 | −4228 | 0.5121320 | 0.00002 | −9.9 |
| 500 | 636 | −4195 | −4430 | −4335 | 0.5121447 | 0.00002 | −9.6 |
| 509 | 647 | −4312 | −4497 | −4414 | 0.5121696 | 0.00001 | −9.1 |
| 518 | 660 | −4462 | −4577 | −4572 | 0.5121498 | 0.00001 | −9.5 |
| 534 | 680 | −4633 | −4798 | −4704 | 0.5121033 | 0.00001 | −10.4 |
| 542 | 692 | −4757 | −4877 | −4836 | 0.5123354 | 0.00003 | −5.9 |
| 548 | 701 | −4829 | −4979 | −4927 | 0.5123008 | 0.00003 | −6.6 |
| 555 | 711 | −4904 | −5084 | −4998 | 0.5121199 | 0.00001 | −10.1 |
| 569 | 723 | −4995 | −5200 | −5059 | 0.5121117 | 0.00002 | −10.3 |
| 581 | 729 | −5052 | −5242 | −5103 | 0.5121198 | 0.00001 | −10.1 |
| 590 | 743 | −5148 | −5328 | −5256 | 0.5122868 | 0.00001 | −6.9 |
| duplicate | | | | | | | |
| 169 | 185 | −327 | −497 | −454 | 0.5120024 | 0.00192 | −12.4 |
| 178 | 198 | −403 | −588 | −544 | 0.5120511 | 0.00230 | −11.4 |
| 196 | 225 | −568 | −698 | −682 | 0.5120082 | 0.00169 | −12.3 |





CPD
9, 2889–2928, 2013

The Misten peat bog (Hautes Fagnes – Belgium)

M. Allan et al.

Title Page
Abstract Introduction
Conclusions References
Tables Figures
◀I ▶I
◀ ▶
Back Close
Full Screen / Esc
Printer-friendly Version
Interactive Discussion

**Table 2.** Results of $^{14}C$ dating for the MIS-08-01b peat core. Independently calibrated age ranges were obtained with the OxCal4 program (Bronk Ramsey, 2009), the modelled ages were obtained after "Bacon" calculations (Blaauw and Christen, 2011). In both cases the IntCal09 calibration curve was used (Reimer et al., 2009).

| Sample Name | Laboratory N° | Depth (cm) | Age $^{14}C$ BP | Modelled age range BC (94.5 % probability) |
|---|---|---|---|---|
| MIS-01/130 | GdA-1545 | 135,5 | 2085 ± 30 | 40–190 |
| MIS-01/153 | GdA-1546 | 142,6 | 2185 ± 35 | 165–375 |
| MIS-01/138 | GdA-1547 | 165,3 | 2240 ± 35 | 200–390 |
| MIS-01/183 | GdA-1548 | 205,5 | 2530 ± 35 | 540–795 |
| MIS-01/202 | GdA-2228 | 228,0 | 2635 ± 20 | 790–825 |
| MIS-01/214 | GdA-2229 | 246,0 | 2440 ± 20 | 405–750 |
| MIS-01/245 | GdA-2230 | 286,17 | 2980 ± 25 | 1125–1305 |
| MIS-01/282 | GdA-2231 | 340,77 | 3470 ± 20 | 1700–1880 |
| MIS-01/334 | GdA-2232 | 408,03 | 3770 ± 30 | 2050–2290 |
| MIS-01/381 | GdA-2233 | 474,25 | 4300 ± 30 | 2880–3010 |
| MIS-01/450 | GdA-2234 | 568,80 | 5050 ± 20 | 3790–3945 |
| MIS-01/476 | GdA-2235 | 603,00 | 5210 ± 30 | 3960–4145 |
| MIS-01/517 | GdA-2236 | 658,80 | 5680 ± 20 | 4460–4545 |
| MIS-01/541 | GdA-2237 | 690,00 | 5940 ± 20 | 4730–4890 |
| MIS-01/589 | GdA-2238 | 741,38 | 6235 ± 20 | 5075–5300 |





CPD
9, 2889–2928, 2013

**Table 3.** Descriptions of testate amoebae zones.

| Zone | Depth (cm) | Calendar Age BC | Major taxa | Zone description |
|---|---|---|---|---|
| 6 | 230–200 | 700–560 | Hyalosphenia subflava | Hyalosphenia papilio and Nebela militaris, Assulina muscorum, Assulina seminulum are variably abundant in this zone. *Amphitrema wrightianum* is nearly absent from this zone. Decrease in *Difflugia pulex* and *Amphitrema flavum* |
| 5 | 370–230 | 1950–700 | *Amphitrema flavum* and *Amphitrema wrightianum* | Decrease in *Difflugia pulex*, *Hyalosphenia papilio* and *Nebela militaris*. *Assulina muscorum*, *Assulina seminulum* are variably abundant in this zone. |
| 4 | 440–370 | 2550–1950 | *Difflugia pulex* | Decrease in *Amphitrema flavum* and *Difflugia* pulex. Increase in *Difflugia pulex*, *Assulina muscorum*, *Assulina seminulum*. Appear *Cyclopyxis arcelloides*, *Hyalosphenia papilio* and *Nebela militaris*. |
| 3 | 550–440 | 3620–2550 | *Amphitrema flavum* | Decrease in *Difflugia pulex*. Variable abundances of *Assulina muscorum*, *Assulina seminulum* and *Difflugia pulex* |
| 2 | 680–550 | 4700–3620 | *Difflugia pulex* | Decrease in *Amphitrema flavum*. Increase in *Difflugia pulex*. Variable abundances of *Assulina muscorum*, *Assulina seminulum* |
| 1 | 750–680 | 5300–4700 | *Difflugia pulex* and *Amphitrema flavum* | Increase in *Difflugia pristis* |





CPD
9, 2889–2928, 2013

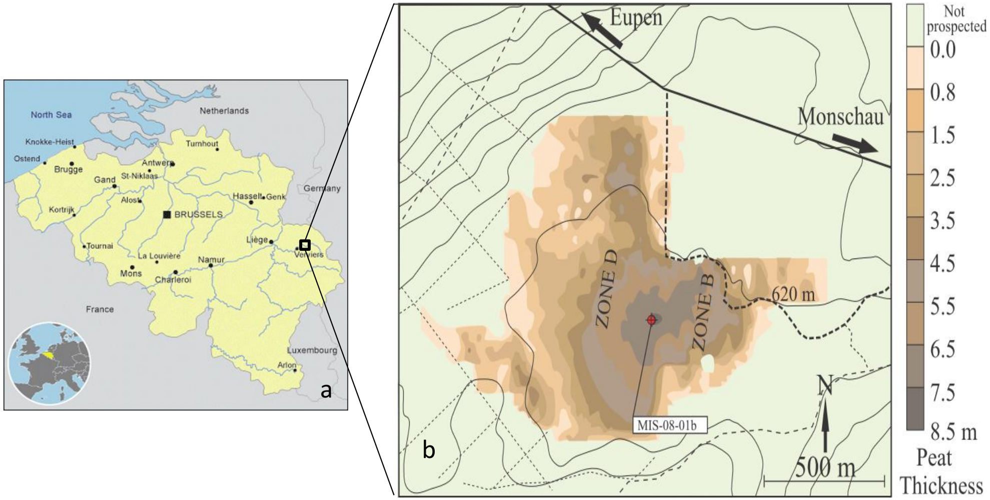


**Fig. 1. (a)** Location of the Misten peat bog in Eastern Belgium and **(b)** map of the Misten peat bog modified from De Vleeschouwer et al. (2007). The colour indicates the peat thickness as deduced from surface radar prospection (Wastiaux and Schumacher, 2003). The red dot shows the location of the MIS-08-01b core.





CPD
9, 2889–2928, 2013

The Misten peat bog (Hautes Fagnes – Belgium)

M. Allan et al.

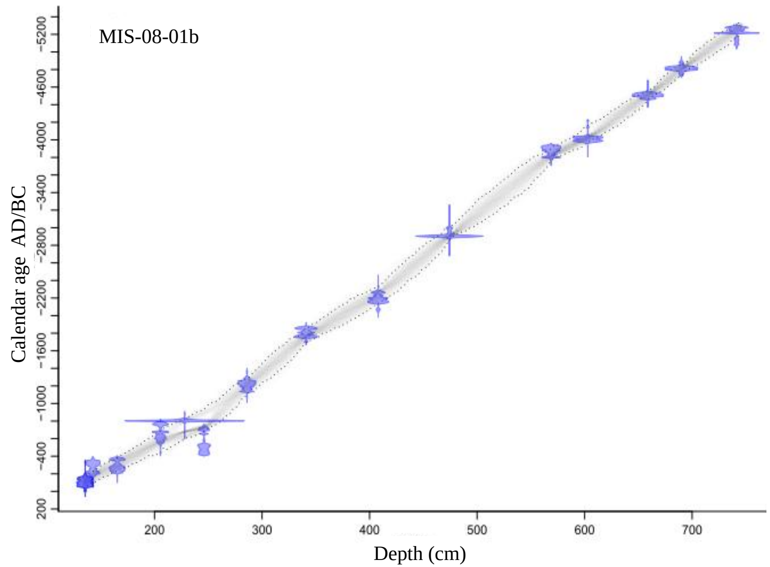


**Fig. 2.** Bacon age-depth model for the MIS-08-01b core. Grey-scales indicate all likely age-depth models, and dotted lines indicate the 95 % confidence ranges.





CPD
9, 2889–2928, 2013

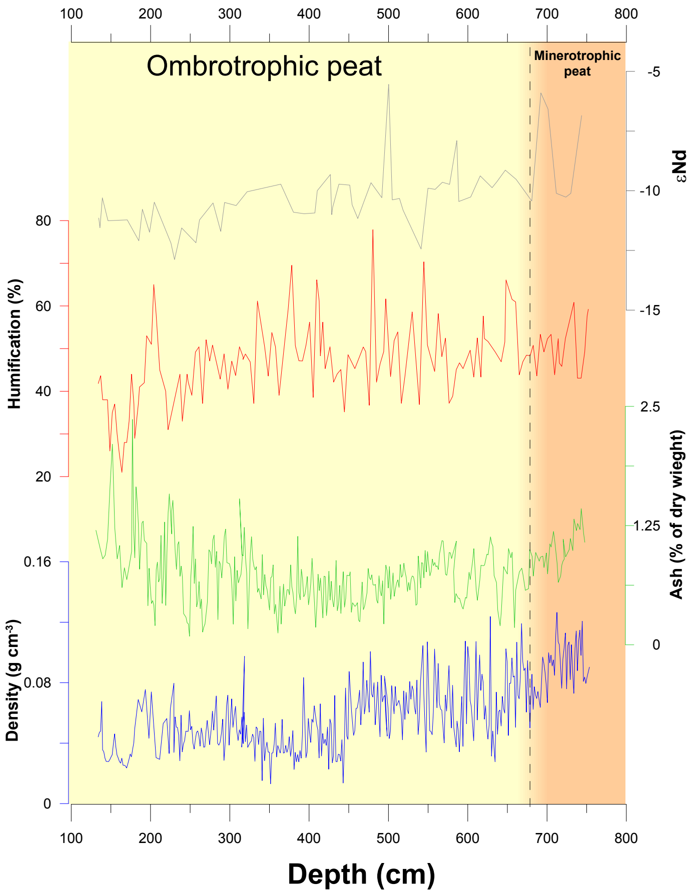


**Fig. 3.** Profiles of bulk density (g cm$^{-3}$), water content (%), ash content (%), and humification (%). Light brown bars correspond to the ombrotrophic peat, and dark brown bar to minerotrophic peat as defined by using Ca/Mg ratios, Sr concentration, and testate amoebae assemblages.





CPD
9, 2889–2928, 2013

The Misten peat bog (Hautes Fagnes – Belgium)

M. Allan et al.

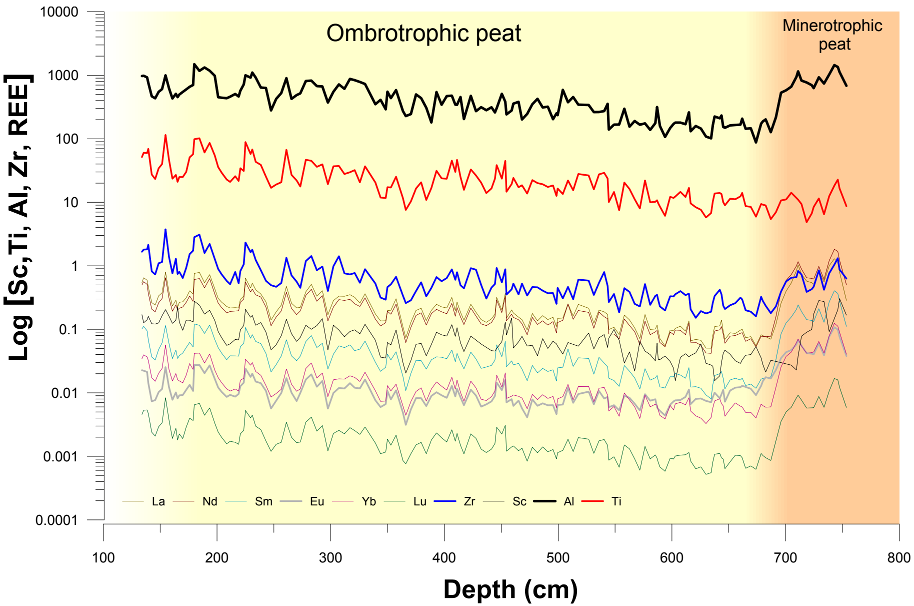


**Fig. 4.** Concentrations of Ti, Al, Sc, Zr, and REE for the MIS-08-01b core. Light brown bars correspond to the ombrotrophic peat, and dark brown bar to minerotrophic peat as defined by using Ca/Mg ratios, Sr concentration, and testate amoebae assemblages.

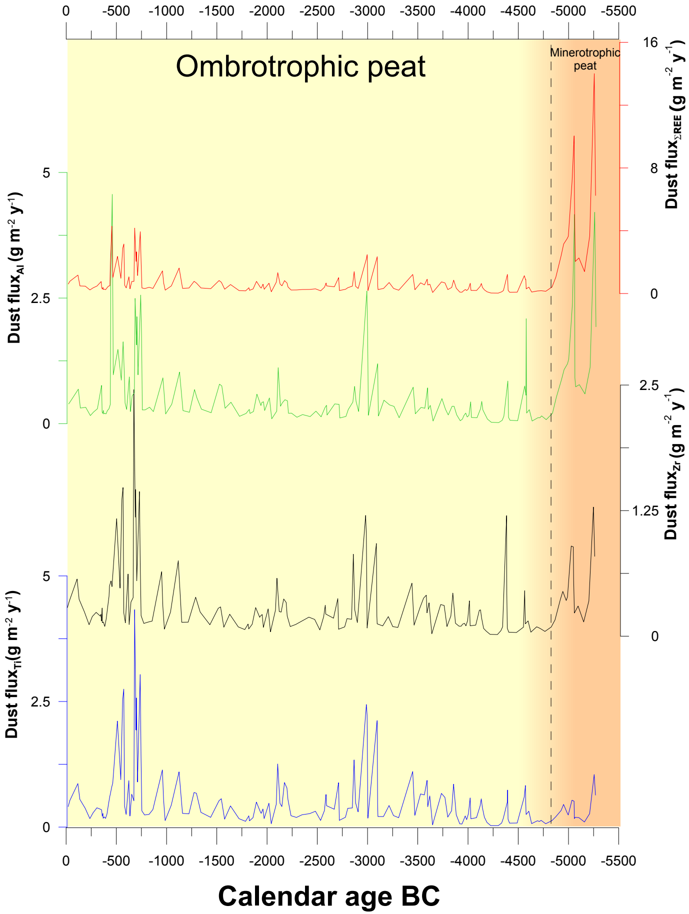


**Fig. 5.** Dust flux given in unit of $g\,m^{-2}\,yr^{-1}$ calculated for Ti, Zr, Al, and $\sum$REE. Light brown bar corresponds to the ombrotrophic peat, and dark brown bar to minerotrophic peat.

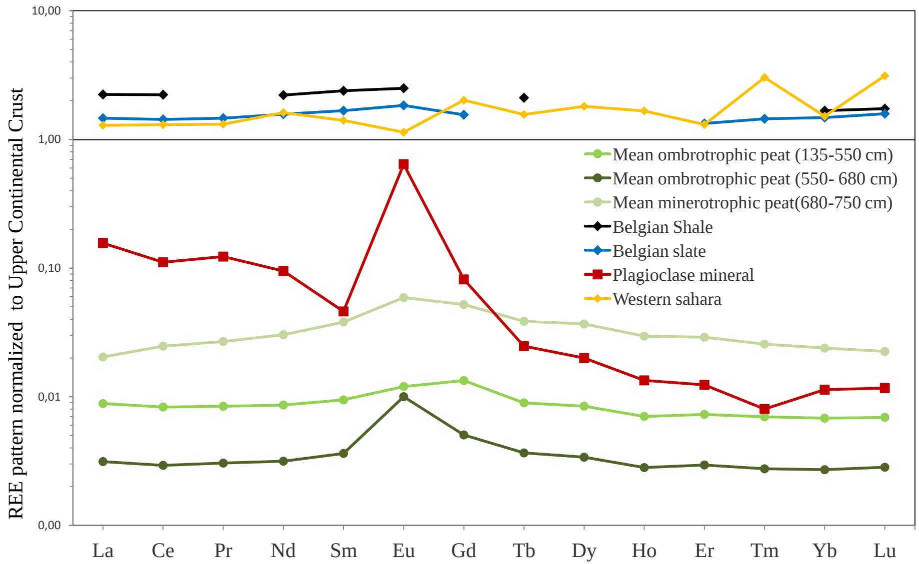


**Fig. 6.** REE average normalized to Upper Crustal Continental (UCC, Taylor and McLennan, 1985) and compared to those obtained from the Western Sahara (Moreno et al., 2006), Germany snow profile (Black Forest, Aubert et al., 2006), Belgian slate (Linnemann et al., 2012), Belgian shales (André et al., 1986), and to those obtained from plagioclase mineral collected in Pan-African rocks (Laouni area, Cottin et al., 1998).





CPD
9, 2889–2928, 2013

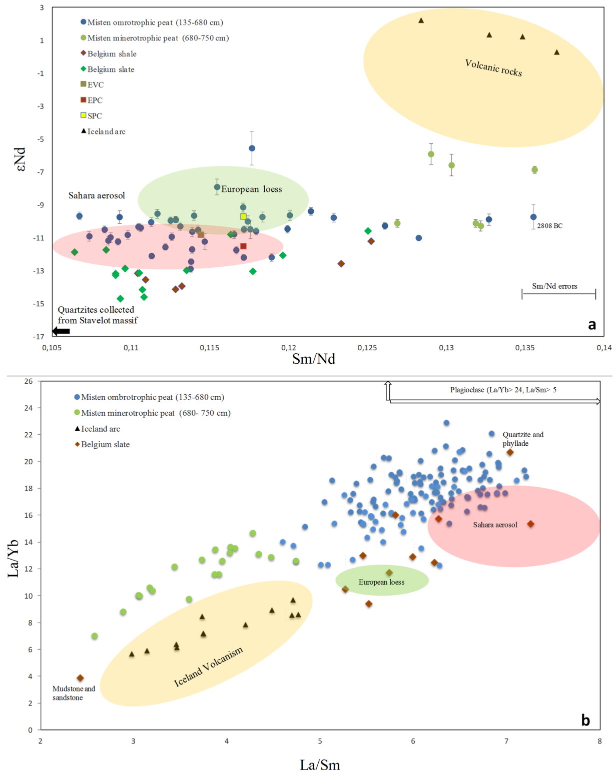


**Fig. 7. (a)** $\varepsilon$Nd vs. Sm/Nd diagram for Misten peat samples. **(b)** La/Yb vs. La/Sm diagram for Misten peat samples. Belgian shale data from André et al. (1986), Belgian slate data recorded from Brabant Massif (Linnemann et al., 2012), Sahara aerosol data from Abouchami et al. (1999) and European loess from Gallet el al. (1998).





CPD
9, 2889–2928, 2013

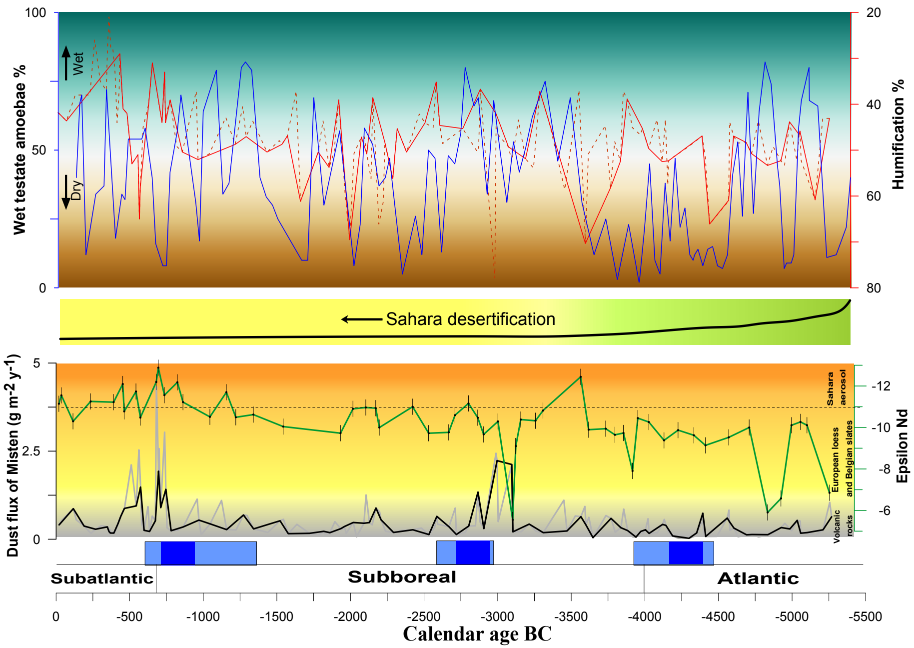


**Fig. 8.** Comparison of the Misten proxy (dust flux, $\varepsilon$Nd, humification, and testate amoebae).The testate amoebae were classified according to their affinity with wet conditions. The three dark blue bars show the cold events representing by Wanner et al. (2011) and the three light blue bars show the length of cold events. Saharan desertification model from Claussen et al. (1999).





CPD
9, 2889–2928, 2013

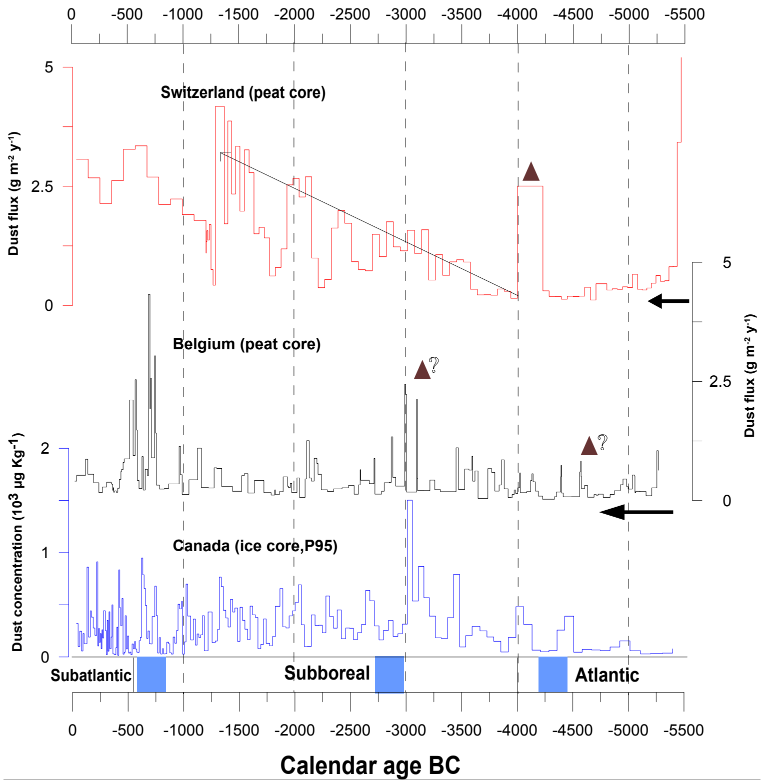


**Fig. 9.** Comparison of the dust flux measured in the Misten bog (black line, this study) with the dust flux ($g\,m^{-2}\,yr^{-1}$) obtained from a Switzerland peat core (green line, Le Roux et al., 2012) and the dust concentration ($10^3\,\mu g\,kg^{-1}$) measured in Canadian ice core recorded from Zdanowicz et al. (2000). The three dark blue bars show the cold events representing by Wanner et al. (2011). Brown triangles represent the volcanic events. Black arrows underline the minerotrophic peat sections.